

See discussions, stats, and author profiles for this publication at: <https://www.researchgate.net/publication/230647865>

Combined ATR-FTIR and DFT study of cyclohexanone adsorption on hydrated TiO₂ anatase surfaces

ARTICLE *in* THE JOURNAL OF PHYSICAL CHEMISTRY C · JULY 2011

Impact Factor: 4.77 · DOI: 10.1021/jp1122129

CITATIONS

12

READS

87

5 AUTHORS, INCLUDING:



M. Calatayud

Pierre and Marie Curie University - Paris 6

86 PUBLICATIONS 1,808 CITATIONS

SEE PROFILE



Frederik Tielens

Collège de France

93 PUBLICATIONS 1,325 CITATIONS

SEE PROFILE



J.A. Moulijn

Delft University of Technology

818 PUBLICATIONS 29,960 CITATIONS

SEE PROFILE



Guido Mul

University of Twente

165 PUBLICATIONS 4,525 CITATIONS

SEE PROFILE

Combined ATR-FTIR and DFT Study of Cyclohexanone Adsorption on Hydrated TiO₂ Anatase Surfaces

Ana Rita Almeida,^{†,||,⊥} Monica Calatayud,^{‡,§} Frederik Tielens,^{||,⊥} Jacob A. Moulijn,[†] and Guido Mul^{*,†,§}

[†]Catalysis Engineering, Delft University of Technology, Julianalaan 136, 2628 BL Delft, The Netherlands

[‡]UPMC Université de Paris 06, UMR 7616, Laboratoire de Chimie Théorique, F-75005, Paris, France

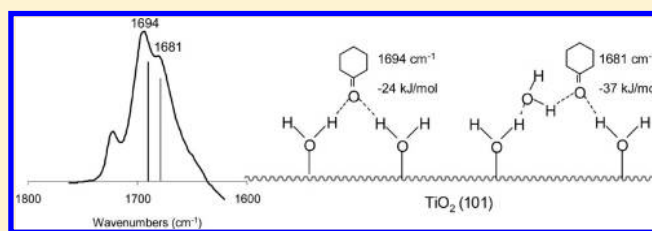
[§]CNRS, UMR 7616, Laboratoire de Chimie Théorique, F-75005, Paris, France

^{||}UPMC Université de Paris 06, UMR 7197, Laboratoire de Réactivité de Surface, F-75005 Paris, France

[⊥]CNRS, UMR 7609, Laboratoire de Réactivité de Surface, F-75005 Paris, France

^{*}PhotoCatalytic Synthesis Group, IMPACT Institute, University of Twente, 7500 AE Enschede, The Netherlands

ABSTRACT: The adsorption of cyclohexanone on different planes ((100), (101), and (001)) of anatase TiO₂, with variable level of hydration, was evaluated by density functional theory (DFT) calculations. Surface hydration was found to affect the cyclohexanone adsorption enthalpy and the calculated infrared absorption frequencies of the preferred adsorbed configurations considerably. A good correlation was found between two experimentally observed absorption frequencies at 1694 and at 1681 cm⁻¹ of cyclohexanone adsorbed on TiO₂, determined by attenuated total reflection Fourier transform infrared (ATR-FTIR), and frequencies calculated for conformations of cyclohexanone interacting with the (101) surface with low and intermediate levels of hydration, respectively. The corresponding adsorption enthalpies of these adsorbed conformations amount to -23.5 and -37.0 kJ/mol, respectively. In addition, DFT calculations show that cyclohexanone physisorption on hydrated (100) yields an adsorption enthalpy of -89.4 kJ/mol. This might be a conformation contributing to irreversible adsorption of cyclohexanone known to occur experimentally after photocatalytic activation of TiO₂. Other phenomena of relevance to irreversible adsorption are also briefly discussed.

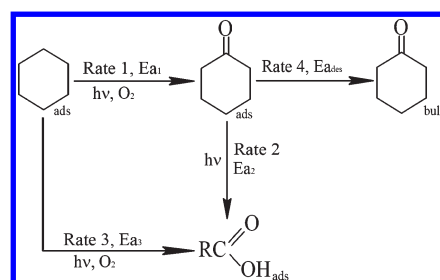


INTRODUCTION

Heterogeneous photocatalysis, in which TiO₂ is most commonly used, enables a large variety of selective mild oxidation reactions, including selective cyclohexane oxidation to cyclohexanone. Photocatalytic reactions are generally operated at room temperature, where product desorption limitations are an issue.¹ Some of us have previously analyzed the selective formation of cyclohexanone by photo-oxidation of cyclohexane over TiO₂, using in situ ATR-FTIR spectroscopy. The various steps of the photocatalytic process are schematically shown in Scheme 1. The desired steps are reactions (1) and (4), whereas carboxylates (undesired) might be formed either directly by unselective oxidation of cyclohexane (reaction 3) or consecutively by oxidation of the adsorbed product cyclohexanone. The latter is likely dominant, since a correlation was found between the rates of desorption of cyclohexanone and accumulation of carboxylates on the catalyst surface, causing deactivation.²

Two carbonyl-related absorption frequencies are always observed for cyclohexanone adsorbed on TiO₂ surfaces. However, the conformation of adsorbed cyclohexanone, and the role of water in determining the adsorption modes, are of relevance in designing TiO₂ surfaces with improved catalytic properties but far from understood. Periodical Density Functional Theory (DFT) calculations can aid infrared spectral interpretation³ and the understanding of interactions between adsorbate and

Scheme 1. Simplified Reaction Scheme of the Cyclohexane Photo-Oxidation



catalyst.⁴ DFT calculations are based on model catalyst surfaces, which usually are very well representative for macroscopic anatase TiO₂ particles, exhibiting 95% of the surface as (101) surfaces, truncated by (001) facets.⁵ However, most commercial TiO₂ catalysts are nanoparticles with a variety of surface facets and defects, like oxygen vacancies, which largely influence the reactivity of the TiO₂ surface.⁶ The large degree of hydration at operating conditions^{7,8} is also of great importance, since the

Received: December 23, 2010

Revised: May 12, 2011

Published: June 05, 2011

adsorption mode of a probe molecule is strongly affected by secondary interactions.⁹ It is possible to approach more realistic conditions in DFT calculations, by introducing a hydration layer on the modeled TiO₂ surface.⁴

In this study the interaction of cyclohexanone with (100), (101), and (001) TiO₂ planes of different hydration levels was studied by periodic DFT calculations, in order to provide further insight in ATR-FTIR spectral interpretation and better understanding on the adsorption conformations of cyclohexanone leading to surface deactivation of TiO₂ during photo-oxidation.

EXPERIMENTAL SECTION

Catalyst Characterization. Solid state ¹H-MAS NMR was performed on a Bruker Avance 400 spectrometer, using a 5 mm zirconia rotor, with spinning speed of 11 kHz. The spectral window was 25063 Hz, with 50 ms acquisition time and 15 s acquisition delay. Transmission electron microscopy (TEM) was performed using a FEI Tecnai TF20 electron microscope with a field emission gun as the source of electrons operated at 200 kV. Samples were mounted on Quantifoil carbon polymer supported on a copper grid, by placing a few droplets of a suspension of ground sample in ethanol on the grid, followed by drying at ambient conditions. The crystal lattice distances were determined by fast Fourier transformation (FFT) of the TEM images, which were generated using Digital Micrograph 3 software.

Cyclohexanone Adsorption Reference. The photocatalyst used in this study was Hombikat UV100 TiO₂ (Sachtleben) of 100% anatase crystallinity (determined by XRD), a *S*_{BET} of 337 m²/g, and a primary particle size of approximately 5 nm.¹⁰ The catalyst was dried at 120 °C for 1 h in static air and suspended in water at a concentration of 1.5 g/L. The suspension was treated for 30 min in a 35 kHz Elmasonic ultrasonic bath; 2 mL of this suspension was spread on a ZnSe crystal and dried in vacuum in a desiccator at room temperature overnight. The coating obtained was dried at 120 °C for 1 h. The thickness of the TiO₂ coating can be estimated considering the theoretical density of the TiO₂ material and knowing the mass of catalyst used in the coating, which leads to a layer thickness of 1.7 μm.

The in situ ATR-FTIR setup used for the cyclohexanone adsorption experiments is described in detail elsewhere.² Cyclohexane 99.0% from Sigma Aldrich and cyclohexanone 99.8% Fluka Analytical were used. Cyclohexane and a solution of 0.05 M of cyclohexanone in cyclohexane were dried over Molsieve (type 4A) overnight before use. A volume of 50 mL of cyclohexane was allowed to flow through the TiO₂ coated ATR cell for 1 h by means of a series II high-performance liquid chromatography pump. After surface stabilization a spectrum was taken as background. For the measurement of the adsorption spectrum for cyclohexanone, the inlet of the ATR cell was switched from pure cyclohexane to the solution of 0.05 M of cyclohexanone in cyclohexane. A Nicolet 8700 spectrometer equipped with a TRS N₂-cooled detector was used. The measurements were done with a mirror velocity of 1.8988 cm·s⁻¹ and a resolution of 4 cm⁻¹. The background and the sample spectra were averaged from 64 and 32 spectra, respectively.

COMPUTATIONAL METHODS

Geometry optimization and molecular dynamics calculations were performed using the ab initio plane-wave pseudopotential approach as implemented in the Vienna Ab Initio Simulation

Table 1. Dimensions of (100), (101), and (001) Unit Cells and Applied Hydration Levels

planes	unit cell dimensions			bare slab thickness (Å)	hydration level (H ₂ O molecules/nm ²)		
	<i>a</i> (Å)	<i>b</i> (Å)	<i>c</i> (Å)				
(101)	7.6	10.9	40	13.8	4.8	9.6	16.8
(100)	7.6	9.5	40	13.1	6.2	9.3	18.5
(001)	7.4	11.6	40	13.3	2.3	7.0	16.4

Package (VASP code).^{11,12} Periodically repeated calculations with the generalized gradient approximation (GGA) density functional by Perdew and Wang PW91¹³ were performed. The valence electrons were treated explicitly, and their interactions with the ionic cores are described by the projector augmented-wave method (PAW), which allows a low energy cutoff equal to 400 eV for the plane-wave basis.

The relaxation of the anatase (100), (101), and (001) planes used in this study was discussed previously.^{14,15} Each surface plane was optimized with different extents of adsorbed H₂O, and the distribution of water layers over the TiO₂ planes was based on previous work by Arrouvel et al.¹⁵ Physisorbed cyclohexanone is stabilized by one or more H-bonds between the oxygen atom of cyclohexanone and a hydrogen atom of a surface active site or adsorbed H₂O molecule. Cyclohexanone was chemisorbed on TiO₂ inducing a chemical bond between a free titanium atom and the oxygen atom of cyclohexanone. The unit cell dimensions were determined for each plane in order to reduce the interaction between adsorbed cyclohexanone with adjacent unit cells. In Table 1 the characteristics of the surface planes with variable levels of hydration and unit cell dimensions are shown.

Geometry optimization calculations were performed with the conjugate-gradient algorithm, at 0 K and at 3 × 2 × 1 k-point mesh and the partial occupancies are set for each wave function using the tetrahedron method with Blöchl corrections.¹⁶ The positions of all the atoms in the supercell as well as the cell parameters are relaxed, in the potential energy determined by the full quantum mechanical electronic structure until the total energy difference between the loops is less than 10⁻⁴ eV.

To explore the surface potential energy of our system, we performed, initially, 0 K geometry optimizations on several intuitive starting configurations; the obtained systems were used as inputs for an ab initio molecular dynamics study within the microcanonical ensemble in the microcanonical (NVE) approach, at *T* = 300 K, to scan the possible conformations of the system. We considered several starting conformations (but no statistics was performed on them), and the run was stopped after *t* ≥ 2 ps. To avoid fluctuations associated to the large time step chosen (2.5 fs), the mass of H atoms was set to 3. The local minima found from molecular dynamics results were systematically reoptimized at 0 K, in order to achieve the absolute electronic minimum energy for each configuration. Molecular dynamics were performed at 1 × 1 × 1 k-points mesh with an energy cutoff of 250 eV.

For both optimization and molecular dynamic calculations, half of the slab was frozen and only the upper four TiO₂ layers were allowed to relax.

Vibrational spectra were calculated, with 1 × 1 × 1 k-points mesh, for a limited number of atoms within the harmonic

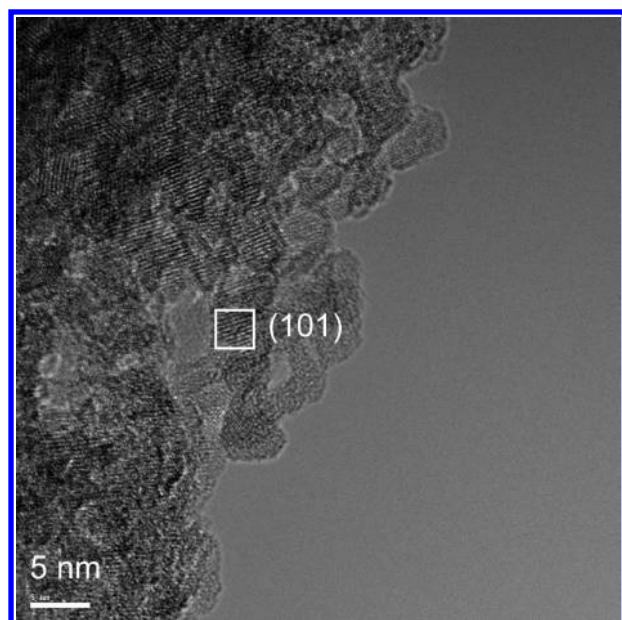


Figure 1. Transmission electron microscopy (TEM) image of anatase TiO_2 UV-100.

approximation. Only the adsorbed cyclohexanone molecule and its neighboring or interacting OH groups on the surface were allowed to move, while the rest of the slab was kept frozen. The eigenvalues of the Hessian matrix after diagonalization lead to the frequency values. The assignment of the vibrational modes was done by inspection of the corresponding eigenvectors. A scaling factor was applied to the calculated carbonyl vibrations. The scaling factor was determined by the ratio between the experimentally observed carbonyl vibration (1722 cm^{-1}) of cyclohexanone dissolved in cyclohexane and the carbonyl vibration calculated by DFT, when the molecule is isolated. This approach is accurate for carbonyl vibrations.¹⁷ Furthermore the scaling factor is dependent on the size of the unit cell (Table 1), so the scaling factor was adjusted for each TiO_2 plane; a similar procedure was successfully undertaken in a previous publication.¹⁸

RESULTS

Catalyst Characterization. Analysis of the applied commercial TiO_2 by X-ray diffraction (XRD) was discussed previously,¹⁹ showing anatase crystallinity, with the diffraction lines of the (101) crystallographic phase being dominant. The bulk crystal-line structure was also analyzed by TEM, as shown in Figure 1. The sample was further analyzed by determination of the lattice parameters, which were calculated by a fast Fourier transformation (FFT). The most common lattice distance in Figure 1 ranged from 0.34 to 0.36 nm, which is indicative of the presence of (101) surface exposed planes.²⁰

The TiO_2 surface is known to be very hydrophilic, being covered with up to three hydrogen bonded water layers.^{21,22} Before photocatalytic activity is determined, a pretreatment at $120\text{ }^\circ\text{C}$ is commonly applied. Thermogravimetric analysis in air reported elsewhere,²³ shows that only 60% of the total amount of adsorbed water is removed by this $120\text{ }^\circ\text{C}$ pretreatment. Under cyclohexane photo-oxidation conditions, the surface hydration is expected to be lower than that obtained under air conditions, but spectroscopic data clearly show the presence of water, remaining

strongly adsorbed on the TiO_2 surface.² Furthermore, water is a byproduct of the photocatalytic cyclohexane oxidation² and is expected to remain adsorbed on the anatase surface. So the effect of strongly adsorbed water on the TiO_2 surface must be considered for interpretation of spectroscopic data. ^1H -MAS NMR measurements on TiO_2 under humid and dried conditions are shown in Figure 2. Under humid conditions (Figure 2a) mainly one narrow peak is visible, corresponding to adsorbed H_2O on the TiO_2 surface. The fact that the peak is narrow suggests a high mobility of the protons measured. Therefore, these are not associated with surface active sites but with layers of adsorbed water on the surface. When the catalyst is heated to $120\text{ }^\circ\text{C}$ (Figure 2b), the NMR signal intensity decreases and shifts slightly to lower fields. The broader signal obtained corresponds to either surface sites or more rigid water molecules with restricted mobility at the surface.⁸

It is known from previous publications²⁴ that the surface—OH sites of anatase TiO_2 show ^1H -MAS NMR peaks at chemical shifts of 2.3 and 6.4 ppm. The high field peak at 2.3 ppm is assigned to basic—OH sites, where the hydrogen atom binds to a terminal oxygen. The low field peak at 6.4 ppm corresponds to the positively charged more acidic protons located on bridged oxygen atoms and forming weak hydrogen bonds with adjacent oxygen atoms.²⁴ The position of the expected OH sites in the NMR spectra is represented in Figure 2b. One main peak is observed which occurs at 5.9 ppm, a similar position as in Figure 2a, corresponding to more rigid molecules of adsorbed water, which can be related to physisorbed H_2O or $\text{Ti—H}_2\text{O}$ sites. The small shoulder around 2.3 ppm, corresponding to basic OH sites, indicate that some of these sites are free. The acidic OH site is not visible, so this site is probably H-bonded to adsorbed water molecules. Weak contributions of bridging and isolated OH sites indicate that they are either occupied by adsorbed water molecules or of low expression in the surface. No explanation was found for the shoulder at 9.8 ppm, which could indicate the presence of a different kind of surface OH site or surface contaminant.

Cyclohexanone Adsorption—ATR-FTIR Spectra. Cyclohexanone adsorption was induced by flowing a solution of 0.05 M of cyclohexanone in cyclohexane for 2 h over the TiO_2 surface. The changes in spectral intensities are shown in Figure 3a. The spectra of externally fed cyclohexanone are similar to those obtained at initial conditions of cyclohexane photo-oxidation,²⁵ which suggests that the adsorption conformations are similar under UV and dark conditions. The range between 1800 and 1600 cm^{-1} contains a band at 1722 cm^{-1} , corresponding to the C=O stretching vibration of dissolved cyclohexanone, as confirmed by the spectrum obtained in the absence of the TiO_2 coating. This study will focus on this vibration, since it is the only cyclohexanone absorption band, which red shifts in the presence of TiO_2 . The two contributions at 1694 and 1681 cm^{-1} correspond to the carbonyl vibration of cyclohexanone when H-bonded to the catalyst surface.² The isosbestic point with positive and negative contributions at 1650 and 1615 cm^{-1} , respectively, is related to a change in the conformation of H_2O adsorbed in the surface, due to cyclohexanone coadsorption. A deconvolution method was applied to different adsorption spectra, and the peak areas of the adsorbed cyclohexanone bands are presented in Figure 3b, as a function of adsorption time. The band at 1694 cm^{-1} is the most prominent; its contribution decreases with a rise in the contribution of the 1681 cm^{-1} peak (Figure 3b). The behavior of these two bands suggests a slow reorganization of cyclohexanone on the surface toward a

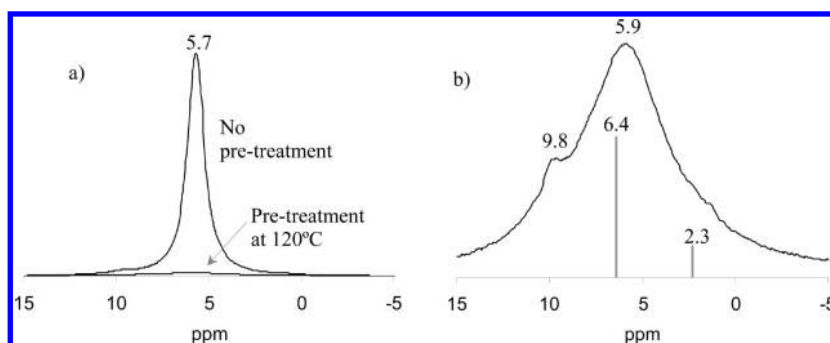


Figure 2. ^1H -MAS NMR of (a) TiO_2 UV-100 with no pretreatment and with a pretreatment of 120°C and (b) focus on the measurement after pretreatment at 120°C . The gray lines correspond to the expected position of TiO_2 active sites.

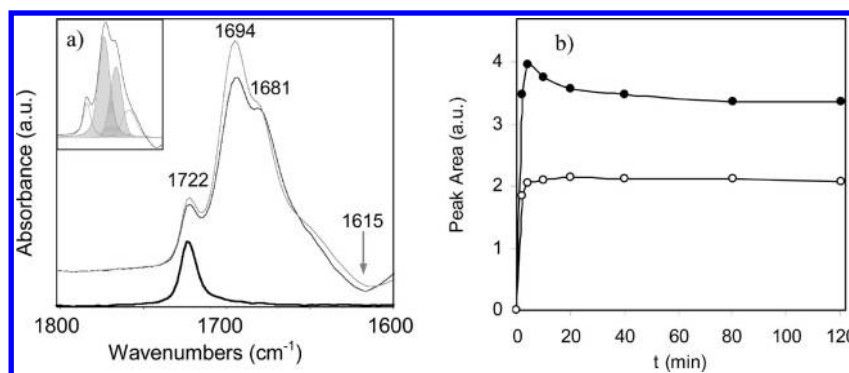


Figure 3. (a) Spectrum of bulk cyclohexanone without TiO_2 (thick black), spectra of 0.05 M of cyclohexanone in cyclohexane adsorbed on TiO_2 (background of cyclohexane adsorbed on TiO_2) for 5 min (gray) and 120 min (black), whose peak deconvolution is shown in the inset. (b) Peak area profile of adsorbed cyclohexanone bands (full black symbols, 1694 cm^{-1} ; empty black symbols, 1681 cm^{-1} , both related to the stretching vibration of the carbonyl group in cyclohexane).

Table 2. Adsorption Energies of H_2O on TiO_2 (100), (101), and (001) at Different Hydration Levels

	(100)	(101)	(001)
Structures			
Hydration ($\text{H}_2\text{O}/\text{nm}^2$)	6.2	4.8	2.3
Energy (kJ/mol)	-68.5	-65.7	-184.7
Structures			
Hydration ($\text{H}_2\text{O}/\text{nm}^2$)	9.3	9.6	7.0
Energy (kJ/mol)	-61.7	-67.1	-97.4
Structures			
Hydration ($\text{H}_2\text{O}/\text{nm}^2$)	18.5	16.8	16.4
Energy (kJ/mol)	-61.0	-57.1	-72.6

preferred adsorption configuration, with a main absorption band at 1681 cm^{-1} . After 120 min the ratio of the 1681 and 1694 cm^{-1} bands is $60/40$.

DFT Calculations. In order to take the effect of adsorbed H_2O on the interaction of cyclohexanone with TiO_2 surfaces into

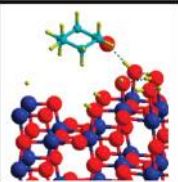
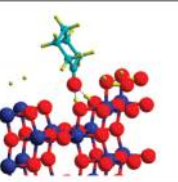
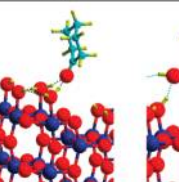
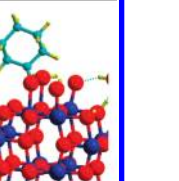
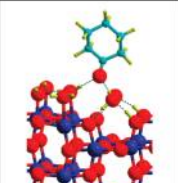
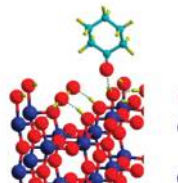
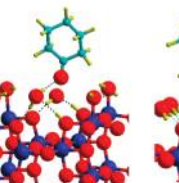
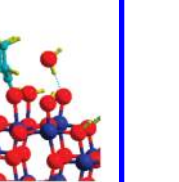
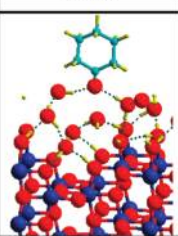
account, TiO_2 surfaces were modeled with different amounts of H_2O molecules adsorbed per nm^2 , as discussed in previous publications.^{15,26} In Table 2 the structures of the (100), (101), (001) TiO_2 surface planes, with different extents of water adsorption, are shown. The lowest hydration level includes only chemisorbed H_2O molecules. The second hydration level includes physisorbed (H-bonded) H_2O molecules on surface OH sites, and the highest hydration level contains an adsorbed water layer. The adsorption energy of a water molecule ($E_{\text{H}_2\text{O,ads}}$ in kJ/mol) on each surface plane and at a specific surface hydration is shown in Table 2. This was calculated according to the equation

$$E_{\text{H}_2\text{O,ads}} = \frac{E_{\text{hydr slab}} - E_{\text{bare slab}} - n_{\text{H}_2\text{O}} E_{\text{H}_2\text{O}}}{n_{\text{H}_2\text{O}}}$$

with $E_{\text{bare slab}}$ corresponding to the calculated energy of the bare (dehydrated) slab, $E_{\text{hydr slab}}$ to the energy of the hydrated slab, $E_{\text{H}_2\text{O}}$ to the energy of one gas-phase water molecule at its equilibrium geometry and $n_{\text{H}_2\text{O}}$ to the number of water molecules added to the unit cell at each hydration level. The negative values presented in Table 2 indicate that the adsorption step is exothermic.

Water chemisorbs on the (100) surface plane at coverages up to $6.2\text{ molecules}/\text{nm}^2$. Some water molecules dissociate on free Ti sites and on bridging $\text{Ti}-\text{O}-\text{Ti}$ sites of a bare (100) surface, with the formation of $\text{Ti}-\text{OH}$ sites and bridging $\text{Ti}-\text{OH}-\text{Ti}$ sites, respectively. Undissociated water molecules chemisorb on free Ti sites and form $\text{Ti}-\text{H}_2\text{O}$ sites. Free $\text{Ti}-\text{O}-\text{Ti}$ sites are also present at the lowest hydration level. Increasing the water coverage to $9.3\text{ molecules}/\text{nm}^2$ leads to water physisorption on

Table 3. Energies (kJ/mol) of Cyclohexanone Physisorption and Chemisorption on the (100) TiO₂ Plane at Increasing Surface Hydration and the Corresponding Conformations^a

Hydration	I	Physisorption II	III	Chemisorption IV
6.2 H ₂ O/nm ²				
OH site Energy Distributio n	Basic OH -48.8 kJ/mol 98.3%	Acidic OH -39.2 kJ/mol 1.7%	Ti-H ₂ O -29.3 kJ/mol 0.0%	Free Ti -15.2 kJ/mol 0.0%
9.3 H ₂ O/nm ²				
OH site Energy Distributio n	Ti-H ₂ O -89.4 kJ/mol 99.9%	Basic OH -70.9 kJ/mol 0.1%	H ₂ O ads. -34.6 kJ/mol 0.0%	Free Ti -51.4 kJ/mol 0.0%
18.5 H ₂ O/nm ²				
OH site Energy Distributio n	H ₂ O ads. -34.0 kJ/mol 100.0%			

^a The probability of the physisorption configuration is determined based on the Boltzmann distribution equation at 25 °C. The preferred configuration at each hydration level is highlighted with a box.

the bridging Ti–O–Ti sites, with a H₂O adsorption energy of –61.7 kJ/mol. The formation of a layered H₂O network is induced at surface hydration levels of 18.5 molecules/nm², characterized by similar affinity of water to the surface, of –61.0 kJ/mol.

On the (101) plane, water chemisorbs without dissociation up to a surface coverage of 4.8 molecules/nm². For this coverage, an adsorption enthalpy of –65.7 kJ/mol was determined with the formation of only Ti–H₂O, leaving bridging Ti–O–Ti oxygen sites still free on the surface. A surface hydration increase to 9.6 H₂O molecules per nm² induces molecular physisorption of H₂O, H-bonded to Ti–O–Ti and neighboring Ti–H₂O sites.²⁶ A decrease in adsorption enthalpy (–57.1 kJ/mol) is observed at higher hydration levels, where a multilayer of adsorbed water is formed.

The (001) surface plane in its bare state (OH free) contains Ti–O–Ti sites with the oxygen atom at a higher plane than the Ti atoms. Upon hydration one of the Ti–O–Ti bonds breaks and two Ti–OH sites are created. Of these two new OH sites, one contains an oxygen atom originally from the TiO₂ lattice structure. Under low surface hydration (2.3 molecules/nm²), the created Ti–OH sites are H-bonded, and free Ti–O–Ti sites are still present.^{15,26} On this TiO₂ plane the energy for dissociative

water chemisorption is much higher (–184.7 kJ/mol). At a surface hydration level of 7.0 molecules/nm² H₂O physisorption occurs, with H₂O molecules H-bridging on the Ti–O–Ti sites, and a reduction of the H₂O adsorption strength to –97.4 kJ/mol. The formation of H₂O multilayers on the surface, at coverages of 16.4 H₂O molecules per nm² is characterized by an adsorption energy of –72.6 kJ/mol.

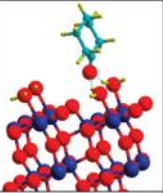
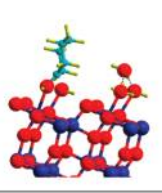
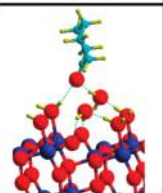
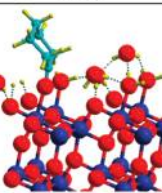
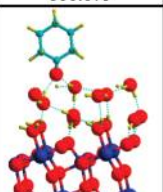
For each surface plane at a specific surface hydration level, the energy of cyclohexanone adsorption ($E_{\text{Cnone,ads}}$ in kJ/mol) is calculated according to the equation

$$E_{\text{Cnone,ads}} = E_{\text{Cnone,hydr slab}} - E_{\text{hydr slab}} - E_{\text{Cnone}}$$

with $E_{\text{Cnone,hydr slab}}$ corresponding to the calculated energy of cyclohexanone adsorbed on a hydrated slab, $E_{\text{hydr slab}}$ the energy of the hydrated slab, E_{Cnone} the energy of the isolated cyclohexanone molecule at its equilibrium geometry with one cyclohexanone molecule per slab ($n_{\text{Cnone}} = 1$). The energy of adsorption of cyclohexanone on different (100) TiO₂ active sites was calculated and is shown in Table 3.

Depending on the surface plane and degree of hydration, different active sites will be available for cyclohexanone adsorption. For TiO₂ (100) surface, three different adsorption sites can

Table 4. Energies (kJ/mol) of Cyclohexanone Physisorption and Chemisorption on the (101) TiO₂ Plane at Increasing Surface Hydration and the Corresponding Conformations^a

Hydration	Physisorption	Chemisorption
4.8 H ₂ O/nm ²		
OH site Energy Distribution	Ti–H ₂ O –23.5 kJ/mol 100.0%	Free Ti –48.9 kJ/mol 0.0%
9.3 H ₂ O/nm ²		
OH site Energy Distribution	Ti–H ₂ O –37.0 kJ/mol 100.0%	Free Ti –31.2 kJ/mol 0.0%
16.8 H ₂ O/nm ²		
OH site Energy Distribution	Ads. H ₂ O –62.1 kJ/mol 100.0%	

^a The probability of each surface conformation is determined based on the Boltzmann distribution equation at 25 °C. The preferred configuration at each hydration level is highlighted with a box.

be considered, and each will present a different adsorption enthalpy for cyclohexanone. Also a chemisorption configuration can be considered, but this was not included in the Boltzmann distribution calculation. The population in the physisorbed configuration of greatest weight depends on the energy of state according to the Boltzmann distribution. For example, the probability of configuration I in Table 3 is given by the relation

$$\frac{\text{configuration I}}{\text{configuration } i} = \frac{\exp\left(-\frac{E_I}{RT}\right)}{\sum_i \exp\left(-\frac{E_i}{RT}\right)} \quad (1)$$

with *i* corresponding to all the cyclohexanone physisorbed configurations (I, II, and III).

For low surface hydration (6.2 H₂O molecules per nm²) three different physisorption sites are available, the basic OH, acidic OH, and Ti–H₂O sites, while chemisorption may occur in the presence of free Ti sites. At room temperature, physisorption on the basic OH of higher adsorption enthalpy (–48.8 kJ/mol) will be energetically favored: the calculations show that 98.3% of the physisorbed molecules have this configuration. The other adsorption configurations, due to their low probability, can be neglected.

For 9.3 H₂O molecules per nm², three possible physisorption configurations can be considered, physisorption on Ti–H₂O sites, basic OH, and an adsorbed H₂O molecule. In this case the preference is toward adsorption on a Ti–H₂O site, with an extra H-bond to a neighboring adsorbed molecule (–89.4 kJ/mol) and the other adsorption configurations can be neglected. So the active sites of preferable adsorption depend on the hydration level. Cyclohexanone adsorption on the (100) TiO₂ plane is enhanced at intermediate hydration levels (9.3 H₂O molecules per nm²), where the adsorption enthalpy of –89.4 kJ/mol is considerably larger than the H₂O adsorption of –61.7 kJ/mol.

At higher hydration levels, direct physisorption of cyclohexanone on the (100) surface is not favored, with the molecule being pushed away from the surface toward to top of the H₂O layer. Therefore only one physical adsorption configuration is possible, which is on the adsorbed H₂O layer of –34 kJ/mol.

The occurrence of cyclohexanone chemisorption is negligible, because its enthalpy, which ranges from 15 to 50 kJ/mol, depending on the hydration level, is lower than the enthalpy for H₂O chemisorption (–68.5 kJ/mol).

The calculated energies for cyclohexanone physisorption and chemisorption on the (101) TiO₂ plane are summarized in Table 4, for different extents of water adsorption. Cyclohexanone physisorption on the (101) at 4.8 H₂O molecules per nm² occurs on the only available active site, Ti–H₂O, with a relatively weak interaction (–23.5 kJ/mol). At a higher hydration level (9.6 H₂O/nm²), the presence of neighboring adsorbed H₂O molecules allows for further stabilization of cyclohexanone physisorption by H-bonding (–37.0 kJ/mol). Direct physisorption of cyclohexanone on a TiO₂ active site at 16.8 H₂O molecules/nm² is not favorable, with the cyclohexanone molecules being pushed away to the top of the water layer, where its adsorption is most stable (–62.1 kJ/mol).

The energy for cyclohexanone chemisorption was determined for the lowest hydration levels only; at high hydration levels it was not favorable. Chemisorption of cyclohexanone shows enthalpies in the same range or even higher than physisorption configurations. However chemisorption is possible only in the presence of a Ti free site, or when the energy for cyclohexanone chemisorption is larger than water chemisorption in this plane (–65.7 kJ/mol). A free Ti site at such conditions will not be preferred due to the high hydration level and cyclohexanone chemisorption is not strong enough to displace H₂O chemisorbed on the surface, so the chemisorption configuration can be neglected at either hydration level.

The calculated energies for cyclohexanone physisorption and chemisorption on the (001) TiO₂ plane are summarized in Table 5, for different extents of water adsorption. For low surface hydrations (2.3 H₂O/nm²), cyclohexanone can physisorb on a Ti–OH site or chemisorb on an existing free Ti site. Energy for physisorption is very weak, below –20 kJ/mol, but the chemisorption energy is considerably high (–78.8 kJ/mol). The (001) plane at low hydration level contains free Ti active sites, so chemisorption will be the preferred configuration. However such low hydration levels are not expected, as demonstrated by ¹H-MAS NMR (Figure 1). At higher hydration level (7.0 H₂O/nm²) no free Ti sites are in the surface, and strong adsorption of water (–184.7 kJ/mol, Table 2) is favorable. At these conditions, H-bridging of cyclohexanone to adsorbed H₂O molecules is the preferred configuration, but the adsorption enthalpy is very low (–12.4 kJ/mol).

ATR-FTIR vs DFT Calculations. The wavenumbers of the vibrations calculated by DFT are usually overestimated, and in

Table 5. Energies (kJ/mol) of Cyclohexanone Physisorption and Chemisorption on the (001) TiO_2 Plane at Increasing Surface Hydration and the Corresponding Conformations^a

Hydration	Physisorption	Chemisorption
2.3 $\text{H}_2\text{O}/\text{nm}^2$		
OH site	Ti-OH	Free Ti
Energy	-19.6 kJ/mol	-78.8 kJ/mol
Distribution	0.0%	100.0%
7.0 $\text{H}_2\text{O}/\text{nm}^2$		
OH site	Ads. H_2O	
Energy	-12.4 kJ/mol	
Distribution	100.0%	

^a The probability of each surface conformation is determined based on the Boltzmann distribution equation at 25 °C. The preferred configuration at each hydration level is highlighted with a box.

order to compare with experimental IR spectra, it is common practice to apply a “scaling factor”. In Table 6, the scaling factors applied for the calculated carbonyl vibrations for each surface plane are presented.

In Figure 4, the calculated spectra of the preferred adsorbed cyclohexanone configurations on the (100) plane with different surface hydrations are compared with the spectra of cyclohexanone adsorbed on TiO_2 , as measured by ATR-FTIR. The spectra calculated for cyclohexanone physisorption show carbonyl vibrations in the region of the experimentally observed vibration at 1681 cm^{-1} . The red shift of the peaks is not proportional to the adsorption strength. The calculated spectra of physisorbed cyclohexanone on TiO_2 (100) with 9.3 H_2O molecules per nm^2 matches best the experimental IR adsorption spectrum. This absorption occurring at higher wavenumbers (1685 cm^{-1}), showed the strongest adsorption enthalpy, -89.4 kJ/mol . Cyclohexanone physisorption on (100) plane with low and high hydration level, occur red shifted in regard to the peaks of the experimental reference. The calculated spectra of chemisorbed cyclohexanone on (100) plane with low and intermediate hydration level occur at 1682 and 1591 cm^{-1} respectively, but are not shown due to the low probability of these configurations.

The spectra of the most stable configurations of cyclohexanone adsorption on (101) TiO_2 , for each hydration level are represented in Figure 5. The calculated carbonyl vibrations for cyclohexanone physisorption on low and intermediate hydration levels are centered at 1690 and 1679 cm^{-1} , which gives a good correlation to experimentally observed peaks (1694 and 1681 cm^{-1}). The band of cyclohexanone physisorption on (101) with $16.8\text{ H}_2\text{O}$ molecules/ nm^2 hydration level, absorbs at lower wavenumbers (1672 cm^{-1}) and does not describe the experimental spectra. Cyclohexanone chemisorption on a (101) plane with low and intermediate hydration levels shows absorption bands at 1679 and 1672 cm^{-1} , respectively, but this kind of configuration is not expected to occur on the surface due to their low probability.

Table 6. Scaling Factor Determined by the Ratio between the Experimentally Observed Free Carbonyl Vibration (1722 cm^{-1}) and the Carbonyl Vibration of an Isolated Cyclohexanone Molecule Calculated by DFT, for Each Unit Cell

	frequency (cm^{-1})	scaling factor
(100)	1738	0.990
(101)	1728	0.997
(001)	1746	0.986

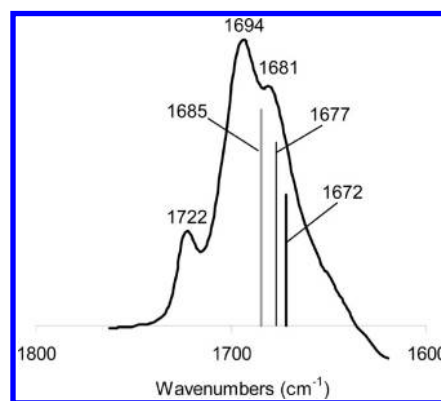


Figure 4. Adsorbed cyclohexanone reference spectrum, measured by ATR-FTIR (thick black spectrum), and the spectra of cyclohexanone physisorbed on a (100) TiO_2 with $6.2\text{ H}_2\text{O}$ molecules/ nm^2 (thick black line), with $9.3\text{ H}_2\text{O}$ molecules/ nm^2 (thick gray line) and with $18.5\text{ H}_2\text{O}$ molecules/ nm^2 (thin black line), as determined by DFT calculations.

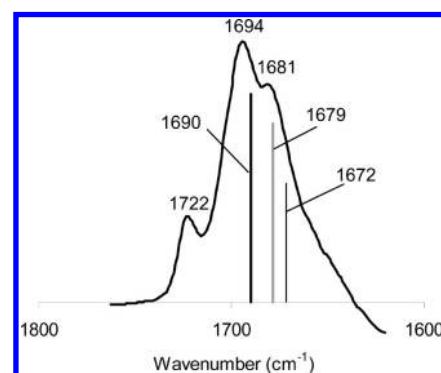
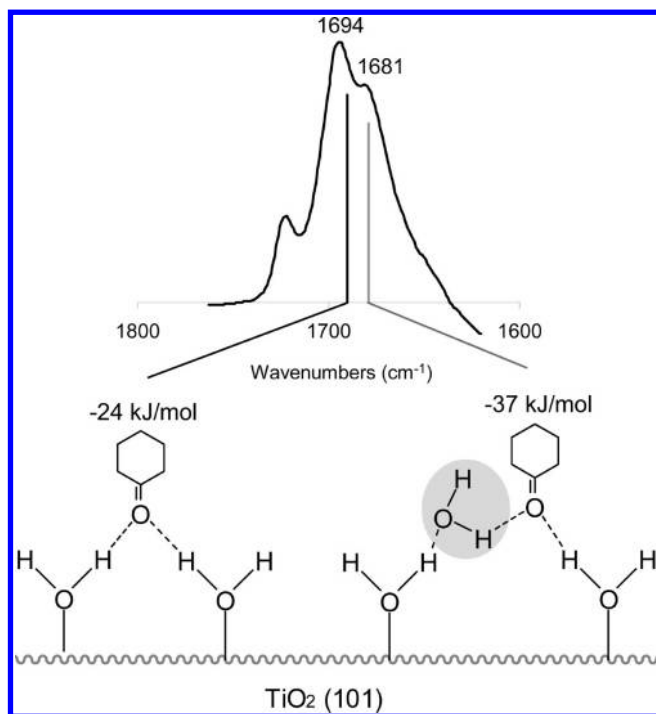


Figure 5. Comparison between an adsorbed cyclohexanone reference spectrum, measured by ATR-FTIR (thick black spectrum), and the spectra of cyclohexanone physisorbed on a (101) TiO_2 with $4.8\text{ H}_2\text{O}$ molecules/ nm^2 (thick black line), with $9.6\text{ H}_2\text{O}$ molecules/ nm^2 (thick gray line), and with $16.8\text{ H}_2\text{O}$ molecules/ nm^2 (thin black line), as determined by DFT calculations.

The calculated spectra of cyclohexanone physisorption on (001) TiO_2 show carbonyl vibrations centered at 1698 and 1682 cm^{-1} . The former band, of cyclohexanone physisorption on (001) plane with $7.0\text{ H}_2\text{O}$ molecules/ nm^2 , is blue-shifted in respect to the experimental spectra. Though the band at 1682 cm^{-1} occurs in the region of the experimental spectra, the adsorption enthalpies are too low (-19.6 kJ/mol) to consider this plane. Cyclohexanone chemisorption on (001) plane with $2.3\text{ H}_2\text{O}$ molecules/ nm^2 also absorbs at 1682 cm^{-1} ,

Scheme 2. Spectral Interpretation of Weak Cyclohexanone Adsorption on (101) TiO₂ Plane with Different Local Hydrations



but given the high chemisorption energy of water on the (001) surface (-184.7 kJ/mol), the presence of free Ti sites is unlikely and so is this conformation of cyclohexanone chemisorption.

DISCUSSION

Structure and Level of Hydration of the TiO₂ Surface.

Before discussing the conformational modes of adsorbed cyclohexanone, we will first address the selection of the surface planes that were taken into consideration. TEM imaging showed that the most common crystalline plane of the anatase catalyst under study (Hombikat UV100) is the (101) plane. However, TEM should be considered as a bulk technique and other less abundant crystal planes may not be clearly resolved. On the basis of literature data, the planes (100) and (001) were therefore also considered in the DFT calculations.^{27,28} Besides the nature of the surface exposed planes, also the respective degree of hydration of these planes is important in determining the interaction with cyclohexanone. The ¹H-MAS NMR study (Figure 2) suggests that the catalyst representative for photocatalytic conversion of cyclohexane contains rigid water molecules on the surface. These can be assigned to physisorbed H₂O or isolated Ti–H₂O sites. Three levels of hydration were therefore taken into consideration in the DFT calculations, i.e., in the ranges of 2–6, 7–10, and 16–18 H₂O molecules nm⁻², the exact value depending on the respective exposed crystal plane.

When evaluating subsequently by DFT the modes of interaction of cyclohexanone with the hydrated surfaces, several sites were taken into consideration (depending on the exposed surface planes these can range from acid to basic sites), of which usually one is highly preferred. This is further discussed in the following.

Spectral Interpretation. In Scheme 2 the spectrum of cyclohexanone adsorbed on TiO₂ is again shown. The presence of two bands assigned to adsorbed cyclohexanone (at 1694 and 1681 cm⁻¹) can originate from different phenomena. First, cyclohexanone might be chemisorbed in certain locations and physisorbed in other locations of the same crystal plane. A very important conclusion is that the DFT calculations show that chemisorption of water on all evaluated Ti sites is much more favorable than chemisorption of cyclohexanone. Therefore cyclohexanone chemisorption can be discarded, as well as this explanation for the presence of two IR bands of adsorbed cyclohexanone. Another possibility to explain the presence of two absorption bands is that physisorption occurs on two different sites. As stated previously the strengths of cyclohexanone physisorption on different available active sites (of similar level of hydration) showed a strong preference toward a specific site with a probability of practically 100%, so also this explanation is not very likely. This leaves two additional explanations for two modes of cyclohexanone adsorption, i.e., (i) the adsorption on different exposed planes or (ii) adsorption on the same plane, which consists of separate areas of different levels of hydration. The first option is not very likely, since the TiO₂ (001) plane interacting with physisorbed cyclohexanone yields very low enthalpies (10–20 kJ/mol, Table 5), which does not agree with the long desorption times observed experimentally.^{23,25} So this plane, if present on the commercial TiO₂ surface, should hardly contribute to the experimentally observed spectra. The best correlation found for the experimentally observed spectra and the calculated values is obtained for the same plane, i.e., the (101) plane, taking into account two local levels of hydration. Although the hydration level is expected to be constant considering the TiO₂ surface globally, the local presence or absence of homogeneously spread physisorbed water induces the two observed cyclohexanone conformations, as shown in Scheme 2. The calculated bands are within 4 cm⁻¹ of the experimental bands, which is a reasonable error for DFT. Cyclohexanone adsorption on a Ti–H₂O active site is of lowest enthalpy (-23.5 kJ/mol) and also of lowest infrared red shift (1694 cm⁻¹). When the TiO₂ hydration level is slightly higher, the adsorption of cyclohexanone on a Ti–H₂O site is stabilized by a neighboring adsorbed H₂O molecule inducing a higher adsorption enthalpy (-37.0 kJ/mol) and consequently a larger IR red shift (1681 cm⁻¹). The latest configuration is preferred but is limited by the presence of adsorbed H₂O molecules. So, it can also be concluded that TiO₂ at experimental conditions exhibits a hydration level between 6 and 9 H₂O/nm², and the free sites available on the surface are probably Ti–H₂O sites.

In previous work the desorption kinetics of photocatalytically formed cyclohexanone was studied.²⁵ Besides reversible adsorption of cyclohexanone, also irreversibly adsorbed cyclohexanone was observed. This is not easy to explain based on the DFT data presented here. Irreversible cyclohexanone adsorption cannot be explained by chemisorption, which is not favorable in the presence of surface hydrated sites. At the same time, even though this surface plane is not experimentally observed, the (100) plane shows very strong physisorption energies of cyclohexanone (Table 3), especially at hydration levels of 9 H₂O molecules per nm² (-89.4 kJ/mol). Furthermore this mode of adsorption would lead to an absorption band of 1685 cm⁻¹, which is observed experimentally. Unfortunately, irreversibly adsorbed cyclohexanone also induces an absorption band at 1694 cm⁻¹, which at present is not completely understood. Other effects may

be influencing adsorption modes of cyclohexanone, like the existence of surface defects, common in TiO_2 catalysts, or an increased surface hydrophilicity caused by UV illumination.^{29,30} However, consideration of these phenomena would require additional advanced DFT calculations. We can conclude based on the presented results that in order to improve cyclohexanone desorption during cyclohexane photo-oxidation, the TiO_2 catalyst should present preferentially the (101) exposed plane, and a low concentration of surface defects.

CONCLUSIONS

To understand the IR features of cyclohexanone adsorption on anatase TiO_2 , different DFT calculations were made, namely, related to physisorption and chemisorption of cyclohexanone on different adsorption sites of (100), (101), and (001) TiO_2 surfaces, with different levels of surface hydration. A good correlation was found between the cyclohexanone adsorption spectra obtained by ATR-FTIR and cyclohexanone physisorption configurations on the (101) surface with low and intermediate hydration levels. The adsorption energies of these conformations are -23.5 and -37.0 kJ/mol, which account for 60% and 40% of the TiO_2 surface, respectively. Stronger adsorption of cyclohexanone could to some extent be related to cyclohexanone physisorption on hydrated (100) planes with a calculated adsorption enthalpy of -89.4 kJ/mol.

AUTHOR INFORMATION

Corresponding Author

*E-mail: G.Mul@utwente.nl.

ACKNOWLEDGMENT

We thank STW, The Netherlands (Project DPC.7065), and the COST action D36, WG No. D36/0006/06 for financial support. This work was performed using HPC resources from GENCI- [CCRT/CINES/IDRIS] (Grant 2009-[x20090820-22]) and the CCRE of Université Pierre et Marie Curie. Thanks to Patricia Kooyman (TUDelft) for the TEM measurements. Thanks to Maria D. Hernandez-Alonso for her contribution to this work.

REFERENCES

- (1) Herrmann, J. M. *Top. Catal.* **2005**, *34*, 49–65.
- (2) Almeida, A. R.; Moulijn, J. A.; Mul, G. J. *Phys. Chem. C* **2008**, *112*, 1552–1561.
- (3) Dzwigaj, S.; Arrouvel, C.; Breyse, M.; Geantet, C.; Inoue, S.; Toulhoat, H.; Raybaud, P. *J. Catal.* **2005**, *236*, 245–250.
- (4) Mendive, C. B.; Bredow, T.; Feldhoff, A.; Blesa, M. A.; Bahnemann, D. *Phys. Chem. Chem. Phys.* **2009**, *11*, 1794–1808.
- (5) Lazzeri, M.; Vittadini, A.; Selloni, A. *Phys. Rev. B* **2001**, *63*, 155409.
- (6) Vittadini, A.; Casarin, M.; Selloni, A. *Theor. Chem. Acc.* **2007**, *117*, 663–671.
- (7) Soria, J.; Sanz, J.; Sobrados, I.; Coronado, J. M.; Maira, A. J.; Hernandez-Alonso, M. D.; Fresno, F. *J. Phys. Chem. C* **2007**, *111*, 10590–10596.
- (8) Nosaka, A. Y.; Fujiwara, T.; Yagi, H.; Akutsu, H.; Nosaka, Y. *J. Phys. Chem. B* **2004**, *108*, 9121–9125.
- (9) Vittadini, A.; Selloni, A.; Rotzinger, F. P.; Gratzel, M. *J. Phys. Chem. B* **2000**, *104*, 1300–1306.
- (10) Du, P.; Moulijn, J. A.; Mul, G. J. *Catal.* **2006**, *238*, 342–352.
- (11) Kresse, G.; Hafner, J. *Phys. Rev. B* **1993**, *48*, 13115–13118.
- (12) Kresse, G.; Hafner, J. *Phys. Rev. B* **1994**, *49*, 14251–14269.
- (13) Perdew, J. P.; Chevary, J. A.; Vosko, S. H.; Jackson, K. A.; Pederson, M. R.; Singh, D. J.; Fiollhais, C. *Phys. Rev. B* **1992**, *46*, 6671–6687.
- (14) Calatayud, M.; Minot, C. *Surf. Sci.* **2004**, *552*, 169–179.
- (15) Arrouvel, C.; Digne, M.; Breyse, M.; Toulhoat, H.; Raybaud, P. *J. Catal.* **2004**, *222*, 152–166.
- (16) Blochl, P. E. *Phys. Rev. B* **1994**, *50*, 17953–17979.
- (17) Tielens, F.; Costa, D.; Humblot, V.; Pradier, C. M. *J. Phys. Chem. C* **2008**, *112*, 182–190.
- (18) Islam, M. M.; Costa, D.; Calatayud, M.; Tielens, F. *J. Phys. Chem. C* **2009**, *113*, 10740–10746.
- (19) Carneiro, J. T.; Savenije, T. J.; Moulijn, J. A.; Mul, G. J. *Phys. Chem. C* **2010**, *114*, 327–332.
- (20) Chemseddine, A.; Moritz, T. *Eur. J. Inorg. Chem.* **1999**, 235–245.
- (21) Soria, J.; Sanz, J.; Sobrados, I.; Coronado, J. M.; Maira, A. J.; Hernandez-Alonso, M. D.; Fresno, F. *J. Phys. Chem. C* **2007**, *111*, 10590–10596.
- (22) Nosaka, A. Y.; Nosaka, Y. *Bull. Chem. Soc. Jpn.* **2005**, *78*, 1595–1607.
- (23) Almeida, A. R.; Carneiro, J. T.; Moulijn, J. A.; Mul, G. J. *Catal.* **2010**, *273*, 116–124.
- (24) Mastikhin, V. M.; Mudrakovsky, I. L.; Nosov, A. V. *Prog. Nucl. Magn. Reson. Spectrosc.* **1991**, *23*, 259–299.
- (25) Renckens, T. J. A.; Almeida, A. R.; Damen, M. R.; Kreutzer, M. T.; Mul, G. *Catal. Today* **2010**, *155*, 302–310.
- (26) Vittadini, A.; Selloni, A.; Rotzinger, F. P.; Gratzel, M. *Phys. Rev. Lett.* **1998**, *81*, 2954–2957.
- (27) Martra, G. *Appl. Catal., A* **2000**, *200*, 275–285.
- (28) Calatayud, M.; Minot, C. *Surf. Sci.* **2004**, *552*, 169–179.
- (29) Sakai, N.; Fujishima, A.; Watanabe, T.; Hashimoto, K. *J. Phys. Chem. B* **2003**, *107*, 1028–1035.
- (30) Fujishima, A.; Zhang, X. T.; Tryk, D. A. *Surf. Sci. Rep.* **2008**, *63*, 515–582.